Binding of Matrix Proteins to Developing Enamel Crystals: An Atomic Force Microscopy Study

Mark L. Wallwork,[†] Jennifer Kirkham,*[,‡] Jin Zhang,[‡] D. Alastair Smith,[†] Steven J. Brookes,[‡] Roger C. Shore,[‡] Simon R. Wood,[‡] Okhee Ryu,[§] and Colin Robinson[‡]

Department of Physics and Astronomy and Astbury Centre for Structural Molecular Biology, University of Leeds, Leeds, United Kingdom, Division of Oral Biology, Leeds Dental Institute, University of Leeds, Leeds, United Kingdom, and University of Texas School of Dentistry, Department of Paediatric Dentistry, 7703 Floyd Curl Drive, San Antonio, Texas 78284-7888

Received September 6, 2000. In Final Form: January 18, 2001

The control of hydroxyapatite crystal initiation and growth during enamel development is thought to be mediated by the proteins of the extracellular matrix. However, the precise nature of these critical mineral−protein interactions remains obscure. In this study, fluid tapping mode atomic force microscopy was used to image, for the first time, the binding of extracellular proteins found in enamel matrix (amelogenin and albumin) to developing enamel crystals. Both albumin and amelogenin were found to be associated with the crystal surfaces under conditions close to physiological; however, the binding of the two proteins was distinctly different. Albumin appeared to bind as a monomer, whereas amelogenin was bound as aggregates resembling previously described "nanosphere" structures. Both proteins were arrayed on the crystal surface in a distinctive banding pattern, perpendicular to the *c*-axis. This pattern was coincident with recently identified positively charged domains on the crystal surface, suggesting that an electrostatic interaction with the net negatively charged proteins controls the proteins' spatial distribution on the mineral surface. Desorption using phosphate buffers of increasing ionic strength indicated that both amelogenin and albumin were tightly bound to the crystals, but amelogenin alone was observed to bind more strongly to certain crystal faces, suggesting a more specific role for this protein in the control of crystal morphology and growth.

Introduction

Dental enamel is the most extreme case of biomineralization and is the only current model in which biological crystals can be obtained for interventive studies with minimum alterations to their surface characteristics. The physical properties of enamel and its physiological function are related to the orientation, morphology, and disposition of the mineral component within the tissue. Calcium hydroxyapatite crystals are the major inorganic component of all mammalian skeletal tissues, but crystals derived from enamel are larger and more uniform than those found in dentine or bone,[1,2] implying a high degree of control during their development. The control of skeletal mineral development (and by implication the onset of calcified tissue pathologies such as osteoporosis and ectopic calcification) is thought to be mediated via the proteins of the extracellular matrix binding to the crystal surfaces and subsequent protein−mineral interactions.

Enamel crystals are initially deposited in a protein-rich matrix within the developing tissue.[3,4] The young (secretory stage) crystals appear as thin ribbons extending from the amelodentinal junction toward the enamel surface, and much of the early crystal growth is elongation in the direction of the crystal *c*-axis.[5] In the later stages of enamel development, protein secretion ceases and matrix degradation reaches a maximum prior to almost complete matrix withdrawal.[6] Matrix degradation and removal is accompanied by increased growth of the crystals in both width and thickness,[7] suggesting a possible inhibitory role for matrix proteins during enamel development. This is supported by in vitro data reported by Robinson et al.[8] which showed that crystal growth did not occur in the presence of enamel matrix proteins.

Enamel matrix proteins comprise a diverse group which includes amelogenins,[9] amelin (ameloblastin/sheathlin),[10] enamelin,[11] enzymes,[12,13] and serum-derived components

* To whom correspondence should be addressed: Professor Jennifer Kirkham, Division of Oral Biology, Leeds Dental Institute, University of Leeds, Clarendon Way, Leeds LS2 9LU, U.K. Tel: 44 (0) 113 233 6156. Fax: 44 (0) 113 233 5158. E-mail: ORL6JEN@ORALBIO.NOVELL.LEEDS.AC.UK.

† Department of Physics and Astronomy and Astbury Centre for Structural Molecular Biology, University of Leeds.

‡ Division of Oral Biology, Leeds Dental Institute, University of Leeds.

§ University of Texas School of Dentistry, Department of Paediatric Dentistry.

(1) Daculsi, G.; Kerebel, B. *J. Ultrastruct. Res.* **1978**, *65*, 163.
(2) Weiner, S.; Price, P. A. *Calcif. Tissue Int.* **1986**, *39*, 365.
(3) Fincham, A. G.; Belcourt, A. B.; Termine, J. D. *Caries Res.* **1982**, *16*, 64.
(4) Simmer, J. P.; Fincham, A. G. *Crit. Rev. Oral Biol. Med.* **1995**, *6*, 82.
(5) Cuisinier, F. J. G.; Steuer, P.; Senger, B.; Voegel, J. C.; Frank, R. M. *Calcif. Tissue Int.* **1992**, *51*, 259.
(6) Robinson, C.; Briggs, H. D.; Atkinson, P. J. *Calcif. Tissue Int.* **1981**, *33*, 513.
(7) Shore, R. C.; Robinson, C.; Kirkham, J.; Brookes, S. J. In *Dental Enamel − Formation to Destruction*; Robinson, C., Kirkham, J., Shore, R. C., Eds.; CRC Press: Boca Raton, FL, 1995; p 135.
(8) Robinson, C.; Kirkham, J.; Stonehouse, N. J.; Shore, R. C. *Connect. Tissue Res.* **1989**, *22*, 139.
(9) Fincham, A. G.; Moradian-Oldak, J. *Connect. Tissue Res.* **1995**, *32*, 119.
(10) Cerny, R.; Hammarstrom, L.; Wurtz, T. *J. Bone Miner. Res.* **1996**, *11*, 883.
(11) Fukae, M.; Tanabe, T.; Murakami, C.; Dohi, N.; Uchida, T.; Shimizu, M. *Adv. Dent. Res.* **1996**, *10*, 111.
(12) Bartlett, J. D.; Simmer, J. P.; Xue, J.; Margolis, H.; Morena, E. C. *Gene* **1996**, *183*, 123.
(13) Simmer, J. P.; Fukae, M.; Tanabe, M.; Yamakoshi, Y.; Uchida, T.; Xue, J.; Margolis, H.; Shimizu, M.; DeHart, B. C.; Hu, C. C.; et al. *J. Dent. Res.* **1998**, *77*, 377.

10.1021/la001281r CCC: $20.00
Published on Web 03/13/2001

such as albumin.[14] Of these, the amelogenins (which comprise approximately 90% of the matrix proteins) and albumin have both been shown to inhibit crystal growth in vitro,[15,16] but very little is known about these protein−mineral interactions or the binding process. It is probable that the binding of enamel proteins such as amelogenin and albumin to developing enamel crystal surfaces is governed by the interaction between specific protein motifs and the crystal surface. In a previous AFM study, we reported that the surfaces of developing enamel crystals carried 30−50 nm domains of positive charge, interrupted by small (∼15 nm wide) areas of negative charge or lower positive charge density, perpendicular to the *c*-axis.[17] Such charge domains may be sites for specific matrix−mineral interactions which control the binding process and therefore play a key role in skeletal tissue mineral development.

There is extensive literature on the adsorption of proteins, particularly serum proteins, to metals,[18−24] glass,[25−30] and polymers.[25,26,30−32] Recently, Kandori et al.[33] reported on a study of serum albumin and lysozyme binding to synthetic calcium hydroxyapatites; however, there have been no reports of the adsorption of proteins to skeletal tissue mineral surfaces and only a few AFM studies of protein binding to related surfaces.[34,35] In a study of protein and peptide binding to calcite, Wierzbicki et al.[35] used AFM and molecular modelling to identify potential binding sites on the mineral surface. The replacement of surface carbonate ions by carboxyl groups on the protein was shown to increase the binding energy significantly, and specific alignment of the oyster shell protein molecules on calcite surfaces was clear in the AFM images.

Atomic force microscopy (AFM) provides an ideal method of investigating protein−mineral binding because imaging can be performed in real time under physiological fluids. These fluids can easily be exchanged during imaging, or proteins can be injected into the fluid cell. The aim of the present study was to use fluid tapping mode AFM to observe the interaction of albumin and amelogenin proteins with developing natural enamel crystals in order to investigate protein−mineral binding and to determine whether protein binding was related to the charge domains recently described on the crystal surfaces.[17]

Experimental Procedures

Source of Material. *Preparation of Enamel Crystals.* Developing enamel crystals, free from all endogenous matrix protein, were obtained from the mandibular incisors of six week old male Wistar rats as described in our previous publications.[36,37]

Proteins Used in Binding Experiments. Bovine serum albumin (BSA) (Sigma U.K.) (MW 65 kDa) was dissolved in 20 mM Tris to a final concentration of 50 μg/mL. The pH of the solution was adjusted to pH 7.4 by titration with small quantities of dilute HCl. Recombinant mouse amelogenin (M 179) (MW 17.9 kDa) representing the full-length nascent amelogenin molecule lacking only the N-terminal methionine and phosphorylation at serine-16[38] was used at a final concentration of 20 μg/mL in 20 mM Tris, pH 7.4.

Atomic Force Microscopy. *Protein−Crystal Binding.* Maturation stage enamel crystals, prepared as described above, were sonicated for 2 min in HPLC-grade methanol to separate aggregated crystals.[37] Approximately 2 μL of this suspension was then placed onto freshly cleaved mica. The methanol evaporated rapidly, leaving a spread of dispersed hydroxyapatite crystals on the surface. Protein solution (either BSA or amelogenin) (20 μL) was then added, and the sample was introduced to the AFM fluid cell in approximately 100 μL of distilled water (pH 7.4). Images were obtained 5 min after addition of the protein.

All samples were imaged on a Digital Instruments Nanoscope IIIa Multimode AFM, equipped with an E type scanner (∼15 μm × 15 μm maximum scan range in the $x-y$ direction) using a commercially available fluid cell (Digital Instruments, Santa Barbara, CA). Tapping mode images were obtained using oxide sharpened silicon nitride NP-S cantilevers of quoted spring constant 0.32 N/m (Digital Instruments U.K., Cambridge) and radii of curvature 5−40 nm. Cantilevers were resonated at approximately 9 kHz, and images were obtained at a tapping amplitude of approximately 80% of free amplitude.

Desorption of Protein from Crystal Surfaces. Desorption of proteins from the crystal surfaces was achieved using increasing strengths of phosphate buffer at pH 7.4.[39,40] Time-lapse images of the crystals were then obtained.

Determination of Surface Roughness. Surface roughness measurements of the crystal and crystal−protein surfaces were obtained using the Nanoscope 4.23 r 3 software where the roughness (R_a) is calculated from the standard deviation of the surface relative to a center plane. The mean roughness in a small area (∼30 nm × 30 nm) was determined, and the average crystal roughness was calculated as the mean roughness over 50 such areas along the crystal surface. Differences in surface roughness measurements were compared statistically using an unpaired *t* test.

Results

Binding of Bovine Serum Albumin to Maturation Stage Enamel Crystals. Figure 1a shows a typical maturation stage enamel crystal in the absence of protein, and Figure 1b shows a typical crystal imaged after the addition of BSA. The protein-free enamel crystals were typically a few hundred nanometers long, 50−100 nm wide, and less than 50 nm high. After the addition of BSA,

(14) Limeback, H.; Sakarya, H.; Chu, W.; Mackinnon, M. *J. Bone Miner. Res.* **1989**, *4*, 235.
(15) Aoba, T.; Moreno, E. C. *Am. Chem. Soc.* **1991**, *444*, 85.
(16) Robinson, C.; Kirkham, J.; Brookes, S. J.; Shore, R. C. *J. Dent. Res.* **1992**, *71*, 1270.
(17) Kirkham, J.; Zhang, J.; Brookes, S. J.; Shore, R. C.; Ryu, O. H.; Wood, S. R.; Smith, D. A.; Wallwork, M. L.; Robinson, C. *J. Dent. Res.* **2000**, *79*, 1943.
(18) Omanovic, S.; Roscoe, S. G. *Langmuir* **1999**, *16*, 5449.
(19) Jackson, D. R.; Omanovic, S.; Roscoe, S. G. *Langmuir* **2000**, *16*, 5449.
(20) Clarke, G. C. F.; Williams, D. F. *J. Biomed. Mater. Res.* **1982**, *16*, 125.
(21) Williams, R. L.; Brown, S. A.; Merritt, K. *Biomaterials* **1988**, *9*, 181.
(22) Hansen, D. C.; Luther, G. W., III; Waite, J. H. *J. Colloid Interface Sci.* **1994**, *168*, 206.
(23) Serro, A. P.; Fernandes, A. C.; Saramago, B.; Lima, J.; Barbosa, M. A. *Biomaterials* **1997**, *18*, 963.
(24) Nanci, A.; Wuest, J. D.; Peru, L.; Brunet, P.; Sharma, V.; Zalzal, S.; McKee, M. D. *Biomed. Mater. Res.* **1998**, *40*, 324.
(25) Brash, J. L.; Davidson, V. J. *Thromb. Res.* **1976**, *9*, 249.
(26) Brash, J. L.; ten Hove, P. J. *Biomed. Mater. Res.* **1989**, *23*, 157.
(27) De Baillou, N.; Dejardin, P.; Schmitt, A.; Brash, J. L. *J. Colloid Interface Sci.* **1984**, *100*, 167.
(28) Brash, J. L.; Uniyal, S.; Chan, B. M. C.; Yu, A. *ACS Symp. Ser.* **1984**, *256*, 45.
(29) Wojciechowski, P.; Brash, J. L. *J. Biomater. Sci.* **1991**, *2*, 203.
(30) Wojciechowski, P.; ten Hove, P. J.; Brash, J. L. *J. Colloid Interface Sci.* **1986**, *111*, 455.
(31) Santerre, J. P.; ten Hove, P. J.; Vanderkamp, N. H.; Brash, J. L. *J. Biomed. Mater. Res.* **1992**, *26*, 39.
(32) Sheller, N. B.; Petrash, S.; Foster, M. D. *Langmuir* **1998**, *14*, 4535.
(33) Kandori, K.; Mukai, M.; Yasukawa, A.; Ishikawa, T. *Langmuir* **2000**, *16*, 2301.
(34) Sikes, C. S.; Wheeler, A. P.; Wierzbicki, A.; Dillman, R. M.; De Luca, L. *Biol. Bull.* **1998**, *194*, 304.
(35) Wierzbicki, A.; Sikes, C. S.; Madura, J. D.; Drake, B. *Calcif. Tissue Int.* **1994**, *54*, 133.
(36) Kirkham, J.; Brookes, S. J.; Shore, R. C.; Bonass, W. A.; Smith, D. A. M.; Wallwork, M. L.; Robinson, C. *Connect. Tissue Res.* **1998**, *38*, 91.
(37) Zhang, J.; Kirkham, J.; Wallwork, M. L.; Smith, D. A. M.; Brookes, S. J.; Shore, R. C.; Wood, S. R.; Robinson, C. *Langmuir* **1999**, *15*, 8178.
(38) Simmer, J. P.; Lau, E. C.; Hu, C. C.; Aoba, T.; Lacey, M.; Nelson, D.; Margolis, H.; Shimizu, M.; DeHart, B. C.; Bartlett, J. D. *Calcif. Tissue Int.* **1994**, *54*, 312.
(39) Gorbunoff, M. *Anal. Biochem.* **1984**, *136*, 425.
(40) Gorbunoff, M.; Timasheff, S. *Anal. Biochem.* **1984**, *136*, 440.

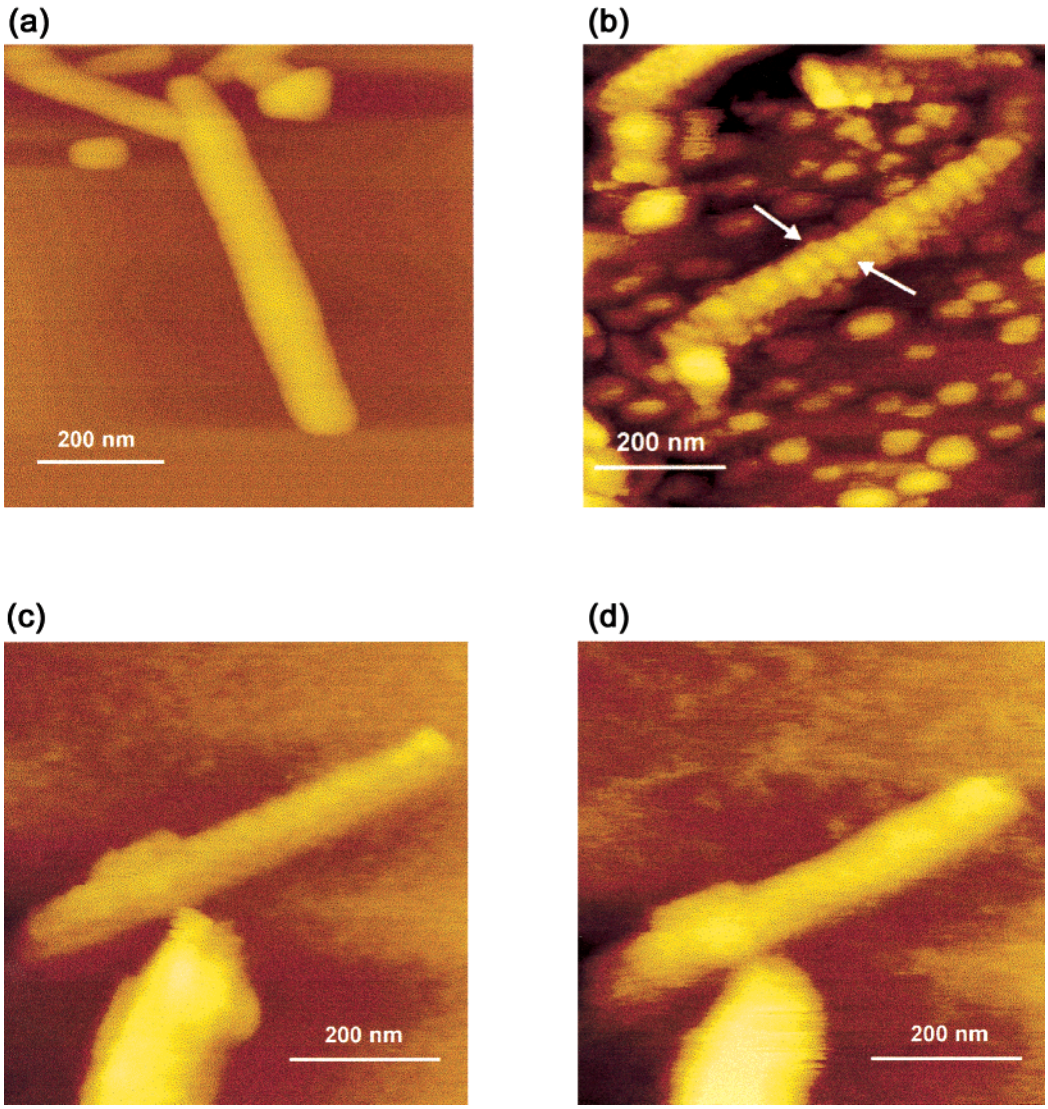

Figure 1. Tapping mode AFM images of maturation stage enamel crystals before and after the binding of BSA and during desorption of the protein from the mineral surface using phosphate buffer. (a) Crystals imaged under distilled water (pH 7.4) prior to the introduction of protein to the fluid cell. (b) Appearance of a typical crystal 5 min after the introduction of protein (20 μL of BSA in 20 mM Tris, pH 7.4, at a final concentration of 50 μg/mL), imaged under a further 100 μL of distilled water. Bands of protein on the crystal surface are visible and are indicated by the arrows. (c) Appearance of a typical crystal 2 min after the exchange of the solution in the fluid cell with 200 mM phosphate buffer. Protein is still visible although the same high definition of the structures as seen in (b) cannot be achieved under the phosphate buffer. (d) Appearance of the same crystal imaged 10 min after the exchange of the 200 mM phosphate buffer in the fluid cell with 500 mM phosphate buffer. There is no evidence for protein remaining on the mineral surface under these conditions.

the AFM images clearly show the presence of globular structures, presumably BSA, associated with both the mica and enamel crystal surfaces. BSA was bound to the crystal surface in a distinct "banding" pattern, with each band perpendicular to the *c*-axis and comprising three to four of the globular structures (arrowed). Measurements made from cross sections along the *c*-axis indicate that the full width at half-height of these globular structures was approximately 20 nm and the height was a few nanometers, which is in broad agreement with the size of monomeric BSA measured by AFM.[41] The structures observed on the mica surface under these solution conditions were considerably larger (75−100 nm in diameter) and presumably correspond to aggregated protein.

Desorption using phosphate buffers is a standard method of removing proteins that are electrostatically bound to surfaces,[39,40] and this technique was used here to study protein desorption from the crystals. Phosphate buffer solutions of two ionic strengths (200 and 500 mM) were introduced into the fluid cell to investigate protein desorption. Figure 1c shows a typical crystal after albumin binding 2 min after the addition of 200 mM phosphate buffer. Figure 1d shows the same crystal 10 min after the introduction of 500 mM phosphate buffer. Under these phosphate buffer conditions, although the protein structures on the crystal surface could be discerned in Figure 1c, they were very much less clearly resolved than in Figure 1b. Surface roughness measurement (R_a) provides a semiquantitative parameter which can be used to make comparisons between the surfaces of protein-free crystals and the same crystals following protein binding and following treatment with phosphate buffers. The roughness of the protein-free and protein-bound crystal surfaces was measured in each of the cases shown in Figure 1, and

(41) Mori, O.; Imae, T. *Colloids Surf., B* **1997**, *9*, 31.

Table 1. Roughness Measurements of Maturation Stage Enamel Crystals before and after Addition of Bovine Serum Albumin and Following Desorption of the Protein with Increasing Strengths of Phosphate Buffer[a]

experimental conditions	surface roughness (nm)
maturation stage crystals in 20 mM Tris, pH 7.4	0.55 ± 0.03
crystals + serum albumin in 20 mM Tris, pH 7.4	1.10 ± 0.08[b]
crystals + serum albumin in 200 mM phosphate buffer, pH 7.4	1.01 ± 0.04[b]
crystal + serum albumin in 500 mM phosphate buffer, pH 7.4	0.59 ± 0.01

[a] Results show mean roughness ± standard deviation; $n = 50$. [b] Significantly different to original crystals in the absence of protein ($p < 0.01$).

the results are summarized in Table 1. These data show that the binding of BSA to enamel crystals is clearly characterized by a statistically significant ($p < 0.01$) increase in the measured roughness. The addition of the 200 mM phosphate buffer resulted in an almost complete removal of the BSA from the mica surface as evidenced by the absence of globular structures, suggesting nonspecific binding of protein. However, there was no significant change in the roughness of the protein-bound crystal surface under these conditions, indicating that the globular (BSA) structures were indeed still present on the crystal surfaces although less clearly resolved by AFM. Addition of 500 mM phosphate buffer resulted in an observable loss of globular structures from the crystals (Figure 1d) and a concomitant decrease in the measured roughness to a value that was not statistically different from that of the protein-free crystals, indicating complete desorption of protein from the crystal surfaces under these conditions.

Binding of Amelogenin to Maturation Stage Enamel Crystals. Similar experiments were carried out to characterize the binding of amelogenin to maturation stage enamel crystals, and the AFM images are presented in Figure 2. Figure 2a shows a typical enamel crystal before introduction of amelogenin protein to the AFM fluid cell, and Figure 2b shows a typical image after the injection of amelogenin. Once again, globular structures can clearly be seen associated with the crystal surfaces in a similar banding pattern to that described for BSA, despite the problem of tip contamination, which is extremely difficult to avoid when proteins are injected into the fluid cell. In contrast to the BSA binding, these images indicated binding of protein aggregates to the crystal surfaces. Each of the globular structures seen measured 25−30 nm in width, which is much larger than would be expected for monomeric amelogenin.

Desorption experiments carried out under the same conditions as those described above for BSA were also performed on the amelogenin−mineral complexes, and the images of this process are shown in Figure 2c,d. The corresponding roughness data are summarized in Table 2. Introduction of 200 mM phosphate buffer into the fluid cell (Figure 2c) resulted in the removal of some proteins from the crystal surface and the almost complete removal of proteins from the mica substrate. The amelogenin also appeared to be more loosely bound to the crystal surface, resulting in displacement of the proteins during scanning. Bound protein aggregates were still clearly visible in Figure 2c, and the measured roughness was not significantly different to that of the crystals before the addition of the phosphate buffer. Introduction of 500 mM phosphate buffer into the fluid cell (Figure 2d) produced different results to those seen with BSA. Protein was removed from the upper surface of the crystal which then exhibited a measured roughness that was significantly reduced compared with the previous measurement ($p < 0.01$) but still rougher than the original protein-free crystals. However, amelogenin aggregates remained closely associated with the sides of the crystal (arrowed), even after prolonged exposure to the phosphate buffer.

Table 2. Roughness Measurements of Maturation Stage Enamel Crystals before and after Addition of M179 Amelogenin and Following Desorption of the Protein with Increasing Strengths of Phosphate Buffer[a]

experimental conditions	surface roughness (nm)
maturation stage crystals in 20 mM Tris, pH 7.4	0.55 ± 0.03
crystals + amelogenin in 20 mM Tris, pH 7.4	1.95 ± 0.10[b]
crystals + amelogenin in 200 mM phosphate buffer, pH 7.4	1.78 ± 0.12[b]
crystal + amelogenin in 500 mM phosphate buffer, pH 7.4	0.82 ± 0.03[b]

[a] Results show mean roughness ± standard deviation; $n = 50$. [b] Significantly different to original crystals in the absence of protein ($p < 0.01$).

Discussion

The results presented here clearly demonstrate the use of AFM in the study of protein−enamel crystal associations. Under conditions of physiological pH, BSA and amelogenin, which are both components of the developing enamel matrix, bind to the natural hydroxyapatite crystal surfaces in an arrangement which corresponds closely to the previously reported charge patterns on these mineral surfaces,[17] suggesting that protein binds to maturation stage enamel crystals in a predetermined pattern dictated by the surface charge distribution.

Our measurements of the size of the bound BSA, although clearly convoluted with the tip shape[42] and possible distortion under the force of the probe, compare with previous AFM studies.[41] In aqueous solution, BSA adopts a prolate ellipsoidal conformation with an 11.6 nm long axis and a 2.7 nm short axis. Our measured width and height (20 nm and approximately 4 nm) are slightly greater than these dimensions but typical for AFM measurements of the protein on a surface. This suggests that BSA binds to the *crystal* surfaces in a monomeric form and not as a large aggregate, examples of which could be seen on the mica surface around the crystal. Such aggregation is not uncommon, but it is perhaps surprising that these aggregates do not appear to adsorb directly onto the mineral surface or onto the first layer of protein. One possible explanation for why this does not occur is that BSA undergoes a conformational change upon binding to the mineral surface which prevents further association with proteins from solution and this conformationally altered state binds preferentially. BSA undergoes a reversible partial unfolding around 316 K,[43] which Jackson et al.[19] have reported increases the tendency to bind to a Ti electrode, and complete thermal denaturation further increased the protein binding in this study. However, at the temperature at which our experiments were performed (297 K) no conformational change of BSA would be expected. Conformational change upon binding is, however, a reasonably well-documented phenomenon; for example, Sheller et al. also observed that albumin formed

(42) Engel, A.; Schoenberger, C. A.; Muller, D. J. *Curr. Opin. Struct. Biol.* **1997**, *7*, 279.
(43) Lin, V. J. C.; Koenig, J. L. *Biopolymers* **1976**, *15*, 203.

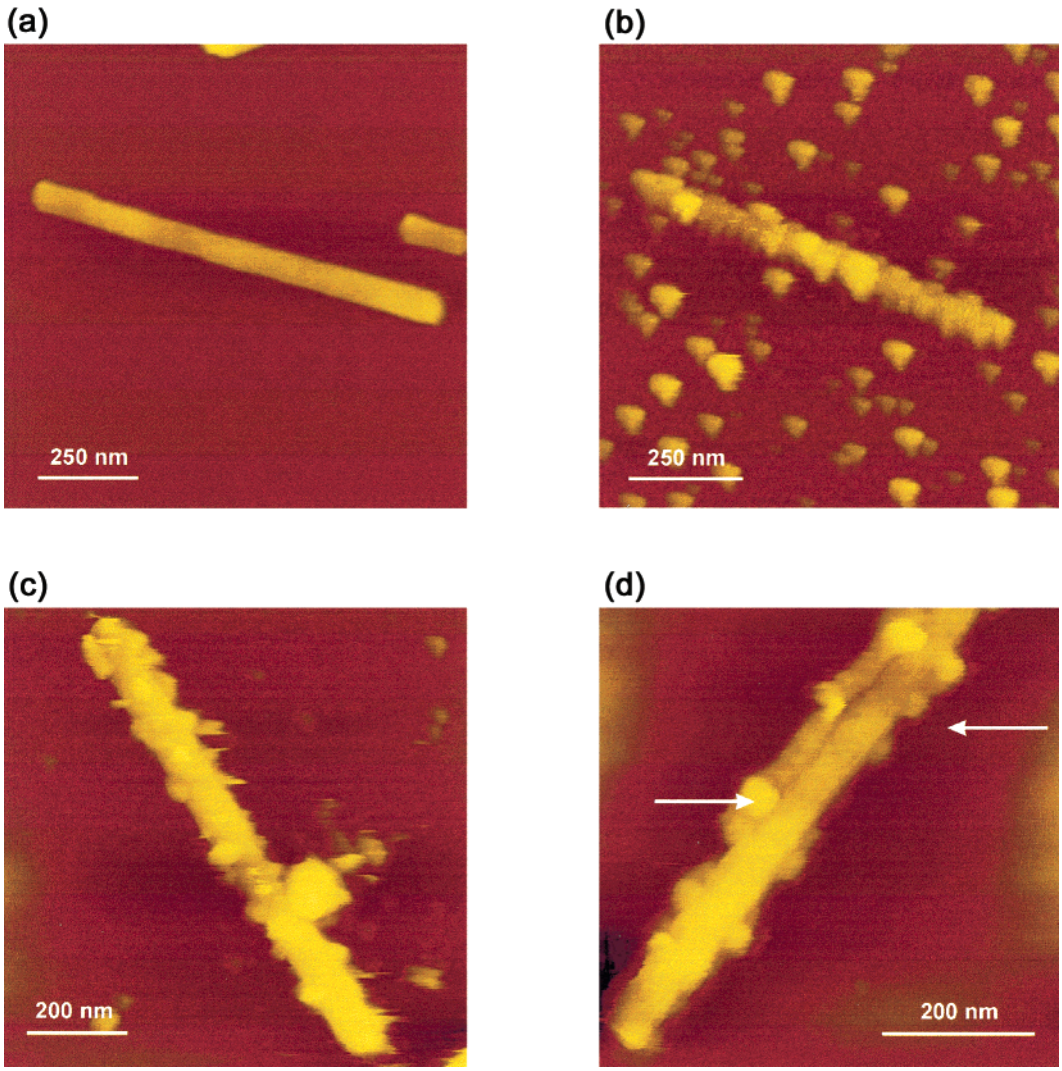

Figure 2. Tapping mode AFM images of maturation stage enamel crystals before and after the binding of M179 amelogenin and during the desorption of the protein from the mineral surface using phosphate buffer. (a) Crystals imaged under distilled water (pH 7.4) prior to the introduction of protein to the fluid cell. (b) Appearance of a typical crystal 5 min after the introduction of protein (20 μL of M179 in 20 mM Tris, pH 7.4, at a final concentration of 20 μg/mL), imaged under a further 100 μL of distilled water. (c) Appearance of a typical crystal 2 min after the exchange of the solution in the fluid cell with 200 mM phosphate buffer. (d) Appearance of the same crystal imaged 10 min after the exchange of the 200 mM phosphate buffer in the fluid cell with 500 mM phosphate buffer. Although the protein has been removed from the upper surface of the crystal, it remains bound to the sides.

exclusively monolayers on a hydrophobic surface[32] and attributed this to conformational changes in the adsorbed protein.

The isoelectric point of BSA is at pH 4.6,[44] and it would therefore be expected to carry a net negative charge at the neutral pH used in these studies. The net surface charge of hydroxyapatite is a subject of conflicting reports in the literature. Previous work, based upon measurements of ζ potential, have claimed both overall positive and negative surface charge for hydroxyapatite crystals.[45] Kandori et al.[33] reported the surface of *synthetic* hydroxyapatite to be negatively charged at pH 6 and suggest that P−OH groups act as surface charge sites. However, there are reports of calcium-rich surface layers on biologically derived crystals that support the view of a net positively charged crystal surface[46] and our own previous work[37] has shown that enamel crystals are immobilized under fluid by binding to negatively charged substrates, providing further evidence that these crystals possess a net positive charge at their surface at neutral pH. We therefore propose that the surface of these *natural* hydroxyapatite crystals comprises large domains of positive charge separated by narrower bands of negative (or less dense positive) charge.[17] Because BSA is net negatively charged at pH 7.4, we suggest that carboxylate groups play the key role in electrostatic binding to the positive domains of this crystal charge motif. Kandori et al.[33] have also postulated that the binding of BSA to synthetic hydroxyapatite was through an electrostatic interaction between the negatively charged BSA and localized positively charged sites on the crystal, so-called C-sites. Rouhana et al. have used electrochemical techniques to study a range of globular proteins including BSA[47] binding to a platinum electrode and have shown that under anodic potentials surface carboxylate groups

(44) Theodre, J. *All About Albumin*; Academic Press: New York, 1996.

(45) Chander, S.; Fuerstenau, D. W. In *Adsorption on and Surface Chemistry of Hydroxyapatite*; Misra, D. N., Ed.; Plenum Press: New York, 1984; p 29.

(46) Mafe, S.; Manzanares, J. A.; Reiss, H.; Thomann, J. M.; Gramain, P. *J. Phys. Chem.* **1996**, *96*, 861.

(47) Rouhana, R.; Budge, S. M.; MacDonald, S. M.; Roscoe, S. G. *Food Res. Int.* **1997**, *30*, 303.

play a major role as the active binding groups. One role of BSA in vivo is to transport Ca^{2+} ions, and these are likely to be abundant in the surface of calcium hydroxyapatite mineral crystals. There may also therefore be an interaction between surface carboxylate groups of the BSA with calcium ions in the mineral surface which mediates the banding pattern of bound protein.

Although albumin is present during enamel crystal development, the most abundant components of the developing enamel matrix are the amelogenins. The data that are presented here suggest that M179 amelogenin binds to enamel mineral crystals in a fundamentally different way than BSA. The measured widths of the globular protein structures observed here (25−30 nm) are not consistent with monomeric protein of this molecular weight. However, the sizes are consistent with previous results describing supramolecular assembly of amelogenin into "nanospheres" in vitro,[49] the observations by electron microscopy of Robinson et al.[50] using freeze-etched developing enamel in vivo, and our preliminary analytical ultracentrifugation data (not shown) which indicates that under these conditions M179 amelogenin forms aggregates which comprise approximately 10 monomers. Amelogenin therefore appears to bind to the mineral surface as an aggregate. This may be a mechanism by which amelogenin increases its binding strength to the crystal surface, that is, by aggregating and therefore increasing the surface area in contact with the mineral.

The isoelectric point of amelogenin is at pH 6.7,[51] suggesting that at pH 7.4 the proteins will carry a small net negative charge. Under these experimental conditions of pH and ionic strength, M179 amelogenin appears to aggregate in solution and the resulting "nanosphere" structures bind to the positive charge present on the enamel crystal surfaces.[52] The additional adsorption of aggregates onto the first mineral-bound protein layer is a further indication of the propensity of this protein to aggregate. Whether there is a conformational change upon aggregation or binding of the aggregates to the mineral is presently unclear, but work is underway to characterize the solution structure of M179 as a monomer and in aggregated form. The binding of amelogenin to the sides of the crystals, even in the presence of 500 mM phosphate buffer, suggests a very strong interaction and a possible mechanism for the control of crystal morphology. In general, proteins appear to bind more strongly to surfaces at pHs near their isoelectric point.[53] Whether this is a general property of proteins is not known, but the increased binding strength of amelogenin at pH 7.4 compared with BSA may be due to the solution conditions being closer to the isoelectric point of M179. Some care must be exercised in discussion of the isoelectric point of proteins in the context of binding to surfaces because it is well-known that the pK_a of chemical groups varies when the groups are in close contact with a substrate. Any conformational changes of the protein which accompany binding are also likely to change which groups are solvent exposed, and these two factors therefore make it highly likely that the isoelectric point of a bound protein is not the same as the solution value. The exceptionally high affinity of the amelogenin "nanospheres" for the sides of the crystal may reflect a difference in crystal surface chemistry and a specific binding of amelogenin, perhaps to sites which correspond to the C-sites identified in synthetic hydroxyapatite as strong binding sites. Modelling has also shown for example that different calcite faces bind proteins with widely varying affinities.[35] The strong binding of amelogenin to the crystal sides could indicate a role for this protein in the observed preferential growth of enamel crystals in the *c*-axis, especially in the early stages of development, when the proportion of the full-length amelogenin molecule (as used in these experiments) is at its greatest within the tissue.

During enamel development, the proteins of the organic matrix, including albumin and amelogenin, are degraded and removed from the tissue by the action of proteases. The data presented here support the theory that failure to remove protein, or ingress of protein (albumin) into the tissue late in development (for example, because of extravasation associated with increased vascular permeability in inflammation), would be expected to result in a failure of crystal growth and subsequent eruption of immature tissue. The resulting clinical appearance would be of a white "chalky" porous enamel which is characteristic of many enamel hypoplasias.[54]

Conclusions

The affinity of both serum albumin and full length amelogenin for maturation stage enamel crystal surfaces at physiological pH conditions, observed here by AFM provides strong further evidence that these proteins are associated with crystal surfaces during enamel development as previously suggested from biochemical studies.[8] The specific binding motif, which reflects the previously reported charge domains on the crystal surface, and the effective removal of protein by phosphate buffer both suggest an electrostatic interaction between the protein and mineral surface. There is some evidence that monomeric BSA adopts a different conformation when bound to the surface but amelogenin exhibits a strong tendency to aggregate in solution before binding to the mineral. The more important role of amelogenin in the control of skeletal mineral crystal morphology and growth is suggested by the specific high affinity of the amelogenin aggregates for the sides of the crystal.

Acknowledgment. The authors thank the Biotechnology and Biological Sciences Research Council of Great Britain (Grant No. 24/9709001) and NIDCR/NIH (Grant No. DE13237) for their support of this work.

LA001281R

(48) Spector, A. A. *J. Lipid Res.* **1975**, *16*, 165.
(49) Fincham, A. G.; Moradian-Oldak, J.; Simmer, J. P.; Sarte, P.; Lau, E. C.; Diekwisch, T.; Slavkin, H. C. *J. Struct. Biol.* **1994**, *112*, 103.
(50) Robinson, C.; Fuchs, P.; Weatherell, J. A. *J. Cryst. Growth* **1981**, *53*, 160.
(51) Sasaki, S.; Shimokawa, H. In *Dental Enamel − Formation to Destruction*; Robinson, C., Kirkham, J., Shore, R. C., Eds.; CRC Press: Boca Raton, FL, 1995; p 85.
(52) Fincham, A. G.; Moradian-Oldak, J.; Simmer, J. P. *J. Struct. Biol.* **1999**, *126*, 270.
(53) Fraaije, J. G.; Norde, W.; Lyklema, J. *Biophys. Chem.* **1991**, *41*, 263.
(54) Small, B. W.; Murray, J. J. *J. Dent. Res.* **1978**, *6*, 33.